Received 6 November 2023; accepted 25 November 2023. Date of publication 5 December 2023; date of current version 30 January 2024.

Digital Object Identifier 10.1109/OJAP.2023.3339368

Sparse Array Mutual Coupling Reduction

C. LARMOUR (Graduate Student Member, IEEE), N. BUCHANAN (Senior Member, IEEE), V. FUSCO (Fellow, IEEE), AND M. ALI BABAR ABBASI (Member, IEEE)

Centre for Wireless Innovation, Queen's University Belfast, BT7 1NN Belfast, U.K.

CORRESPONDING AUTHOR: C. LARMOUR (e-mail: clarmour04@qub.ac.uk)

This work was supported by the Department for Education. The work of M. Ali Babar Abbasi was supported in part by the European Union Horizon 2020 Project 6G-SANDBOX through UKRI under Grant 101096328, and in part by the Department for the Economy of Northern Ireland through U.S. Ireland R&D Partnership under Grant USI 199.

ABSTRACT This paper provides a concise overview of recent developments in sparse antenna arrays, with a specific focus on techniques for reducing mutual coupling. It explores the concept and definitions of sparse arrays in different applications, highlighting their historical significance in antenna theory. The paper addresses the mutual coupling problem and presents reduced coupling geometrical configurations through illustrative examples. Various mutual coupling compensation techniques are discussed. The paper conducts a comprehensive comparison of multiple array design optimisation techniques, including genetic algorithm, covariance matrix adaptation evolution strategy, particle swarm optimisation, trust-region framework, Nelder-Mead simplex algorithm, interpolated Quasi-Newton, and classic Powell. The comparison emphasizes achieving desired radiation performance and evaluates the mutual coupling coefficient using 4×4 planar arrays and 16×1 linear arrays with typical patch antennas in the mmWave bands. Notably, the paper considers optimised non-uniform antenna element positioning within the arrays, which has shown promising results in reducing mutual coupling. The study also introduces the application of beam steering to these optimised non-uniform arrays, demonstrating resilience to beam steering degradation and potential performance improvements. The findings indicate that particle swarm optimisation generally provides the most consistent performance across the discussed optimisation problems.

INDEX TERMS Algorithms, antenna arrays, antenna array mutual coupling, mutual coupling, optimization methods, sparse array antennas.

I. INTRODUCTION

SPARSE antenna arrays are revolutionizing the field by offering a groundbreaking approach to multi-antenna systems. Unlike traditional arrays, sparse arrays are meticulously crafted to have a significantly reduced number of elements, resulting in a remarkable reduction in cost and complexity without compromising crucial performance metrics such as radiation pattern, gain, and beam width. Their versatility extends across diverse domains, encompassing radar, satellite communication [1], and the burgeoning realm of wireless communication [2]. While conventional array geometries like uniform linear arrays (ULAs) and uniform rectangular arrays (URA) have long been employed, sparse arrays have emerged as a game-changer, effectively eliminating the redundancy stemming from inter-element spacing inherent in ULAs. The extensive literature surrounding sparse arrays reflects their wide-ranging designs and applications, demonstrating their prowess in achieving comparable resolution with a markedly reduced number of elements. Fabricated sparse antenna arrays can be seen in Fig. 1. These cited works display just a few of the various fields to which the sparse array methodology can be applied to improve performance and reduce hardware costs.

Although sparse arrays inherently exhibit reduced mutual coupling compared to ULAs, it is imperative to acknowledge that mutual coupling still demands careful consideration. This is particularly relevant in cases where closely spaced portions of sparse arrays or novel designs incorporate ULAs. Neglecting mutual coupling can have detrimental effects on array performance [3]. Extensive research has yielded a plethora of sparse array designs that effectively mitigate mutual coupling by leveraging increased inter-element

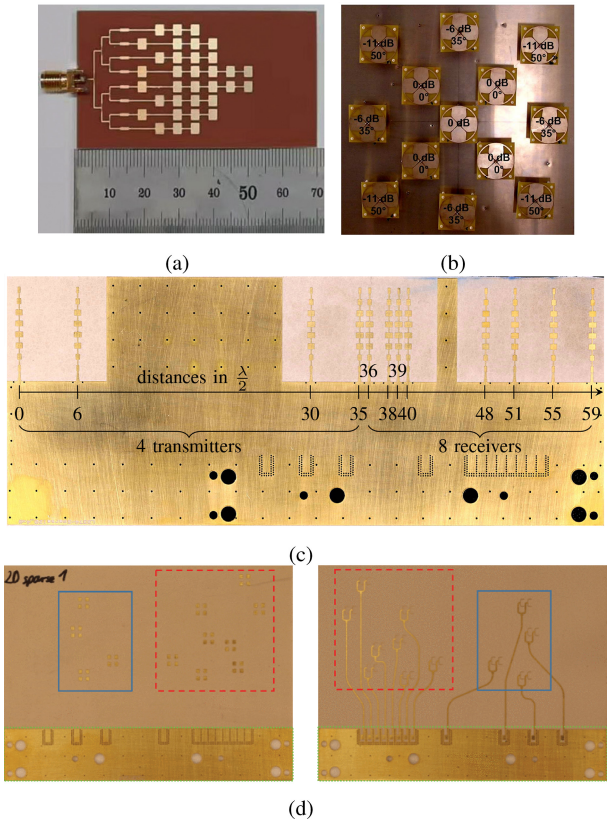

FIGURE 1. Sparse array designs for (a) 5G wireless communication [4]. (b) Radar cross section measurements using cross entropy optimisation [6]. (c) Compressive sensing direction-of-arrival estimation [5]. (d) 2D Multiple-Input-Multiple-Output radar systems [7].

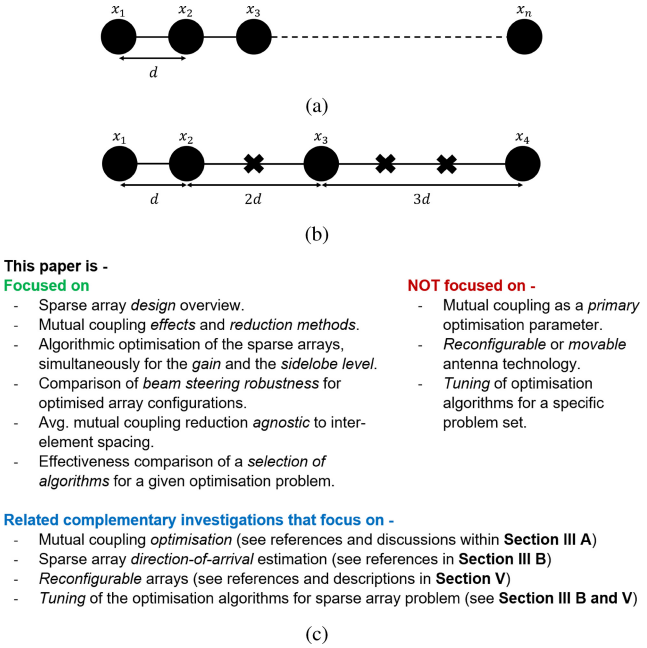

FIGURE 2. (a) ULA diagram showing element spacing. (b) Sparse array diagram showing element spacing. (c) Visual summary of the topics covered in the paper.

spacing. Furthermore, some studies have explored the optimisation of mutual coupling matrices (MCMs) to minimize these effects. This paper not only reviews these mutual coupling reduction methods comprehensively but also proposes application-specific strategies for mitigating mutual coupling within the field. Furthermore, this work introduces a novel approach to sparse array design, considering non-uniform element positioning within the arrays and the application of beam steering to these non-uniform arrays, factors that have been overlooked in previous studies. The comparison emphasizes achieving desired radiation performance and evaluates the mutual coupling coefficient using 4×4 planar arrays and 16×1 linear arrays with typical patch antennas in the mmWave bands. The sparse antenna arrays in this paper are comparable to the designs shown in Fig. 1, showcasing the possibility of applying the optimisation methodologies across a wide range of applications.

The structure of the paper is outlined as follows: Section II provides a concise overview of sparse arrays, encompassing both linear and 2D configurations. It explores the diverse array designs employed in these areas. Section III delves into the crucial topic of mutual coupling within sparse arrays. It highlights the impact of mutual coupling on array performance and examines designs that exhibit reduced mutual coupling. Additionally, this section explores algorithms and optimisation techniques utilized to mitigate the effects of mutual coupling. Section IV presents simulation results showcasing the optimisation outcomes for different array geometries. These results serve to demonstrate the suitability of the employed algorithms in achieving the desired objectives. Section V initiates a general discussion surrounding the obtained results, and it identifies potential avenues for future research within the field. Finally, the paper concludes by summarizing the key findings and contributions in Section VI. A visual summary of the topics covered within the paper is shown in Fig. 2 (c).

II. SPARSE ARRAY OVERVIEW

A diagram for a ULA can be seen in Fig. 2 (a) with N elements with inter-element spacing d which is equivalent to half of wavelength ($\lambda/2$) or less [8]. This allows the ULA to provide a resolution of $N-1$ sources. Linear sparse arrays are considered appealing as they allow for a reduction in the number of elements, when compared with a ULA within an array while allowing for the same resolution to be achieved, i.e., they have a resolution of $N-1$ with less than N elements in the array. Inter-element spacing is also increased which, in turn, leads to reduced mutual coupling effects. Sparse array element spacing is notated as a, b, c with $n-1$ entries for an n-element array. So for example an array notated as $1, 3, 6$, so this array has 4 elements with placements at $0, 1, 3, 6$ as shown in Fig. 2 (b) and the positions with crosses show locations without any elements.

First, let's look at various types of sparse arrays that have differing designs and properties when compared. Minimum redundancy arrays (MRAs) are based on ULAs and involve removing selected elements that allow the array to maintain

the same resolution while reducing the number of active elements [9]. Another name used for such array configuration is the minimum hole arrays (MHAs). 'Hole' means a missing antenna element in the co-array. They are similar to MRAs in that they have no closed-form expression for element positions, however, they differ in that antenna positions are optimised so that a given spatial lag is only obtained once [10]. Co-prime arrays consist of two ULAs spaced more than half a wavelength apart and allow for a greater number of degrees-of-freedom (DOFs) than a ULA [11], [12]. Another widely used and discussed term that is relevant to sparse arrays is the *nested arrays*, which are produced using two ULAs and produce a hole-free difference co-array (DCA) [13] therefore making them preferable to co-prime arrays, which are not hole free. Nested arrays can also be considered as an alternative to MRAs with the added benefit of having a closed-form expression for element placements. Building on this, the super nested array (SNA), takes the nested array design which is more susceptible to mutual coupling, and re-configures the element positioning so the effects of mutual coupling are reduced [14]. A full review of sparse arrays is outside the scope of this paper and more in-depth reviews are readily available. Linear sparse arrays are documented in [15], where varying types of sparse arrays are discussed along with the properties and equations. Sparse phased array structures are examined with greater depth in [16], covering both theoretical explanations and practical applications. Novel array architectures including both sparse and thinned arrays are covered in [17]. Lastly, a review of 2D direction-of-arrival (DOA) estimation provides a comprehensive overview of existing 2D sparse array designs. This includes properties of these arrays including a number of sensors, DOFs, etc. Some details regarding algorithms used by sparse arrays are also included. This paper also documents the performance of arrays in regard to mutual coupling and denotes how some arrays are less subject to mutual coupling effects [18].

III. MUTUAL COUPLING

A. MUTUAL COUPLING EFFECTS

Mutual coupling is a complex phenomenon that refers to the interaction between the elements of an array antenna and can have a significant impact on the overall performance of the array [19]. This interaction can manifest in different ways, such as changes in the radiation patterns, gain, and directivity of the array, as well as changes in the phase relationships between the elements. Understanding and controlling mutual coupling is crucial for array systems, particularly in DOA estimation applications, which are widely used in radar and communication systems [3]. Moreover, mutual coupling can also affect subchannels in Multiple-Input-Multiple-Output (MIMO) systems, depending on the array configurations and the environment [20].

Sparse arrays, which have a large inter-element spacing, are often considered to be less affected by mutual coupling effects [21]. However, this assumption is not always correct, as neglecting to account for mutual coupling can lead to reduced performance [21], [22]. Studies have shown that uniform linear arrays (ULAs) are the most affected by mutual coupling, while minimum redundancy arrays (MRAs) are the least affected, due to the inter-element spacing of the arrays [23]. In addition, the type of antenna used in the array can also affect mutual coupling. Microstrip antennas, for example, have been shown to be more affected by mutual coupling than dipole antennas [22]. Furthermore, mutual coupling can be dependent upon whether the array is transmitting or receiving, and mutual impedances within the array should be modelled as such for analysis [24]. Clearly, it is important to take into account mutual coupling in the design and optimisation of array antenna systems to ensure optimal performance and accurate results. This is crucial as we transition from simple multi-antenna systems to massive MIMO systems, and now to extremely large antenna arrays for future communication systems.

B. REDUCED MUTUAL COUPLING DESIGNS AND OPTIMISATION TECHNIQUES

Numerous sparse array designs, based on concepts like MRAs, co-prime arrays, and nested arrays, have modifications for performance optimisation. Let's first discuss a few examples of such designs. The super nested array (SNA) and its generalized version, the Q^{th}-Order super nested array, refine the standard nested array design, achieving lower mutual coupling effects [25]. Another design, the sparse nested spatially spread orthogonal dipole array (SNODA) is a nested array design and the distance between sensors is much larger than half-wavelength, which allows for the reduction of mutual coupling within the array while offering improved spatial resolution without extra sensors or elements [26]. In terms of co-prime arrays, designs such as padded coprime arrays (PCAs) increase DOFs and reduce mutual coupling through structural adjustments and greater inter-element spacing [27]. Other designs like unfolded parallel coprime arrays (UPCA) and augmented nested coprime array with displaced subarrays (ANCADiS) model share similar enhancements [28]. Lastly, 2D sparse array designs have been introduced with larger element spacing and increased DOFs for reduced mutual coupling in [29], proposing new planar sparse array designs with hole-free co-arrays, and spacing between the elements is greater which in turn reduces mutual coupling. Designs include half-open box arrays, half-open box arrays with two layers and hourglass arrays, which are all variations on planar arrays with differing element configurations. Hourglass arrays are reported to have the best performance against mutual coupling out of the proposed designs. Modified hourglass designs have also been proposed that can identify an increased number of sources [30]. Another notable approach is the deterministic synthesis proposed in [31], which emphasizes achieving the desired radiation pattern with a reduced number of antenna elements, this is achieved using an approach termed the Array Dilation Technique (ADT) which stretches the array, similar to an

elastic membrane, creating aperiodicity. The technique does not require any model taper and starts with a uniformly fed array with uniform spacing. The ADT demonstrates lower sidelobe levels (SLL) for optimal thinning levels compared to previous literature. This method provides a systematic way to design sparse arrays, ensuring optimal performance without the need for exhaustive iterative processes.

Alternative methods for reducing mutual coupling in sparse arrays include iterative and simultaneous approaches that compensate for mutual coupling, as suggested by [22]. An optimisation framework is introduced in [21] that overcomes design limitations of ideal antenna elements. A robust DOA estimation method under unknown mutual coupling, producing co-array signals with less mutual coupling, is proposed by [32]. This technique uses a joint sparse recovery for DOA estimation and offers similar performance to LASSO with compensation. Optimisation algorithms can refine the element spacing in sparse arrays and mitigate mutual coupling. In [30] simulated annealing (SA) was utilised to enhance the hourglass design performance. Nature-inspired optimisation algorithms in non-uniform arrays are evaluated in [33], including covariance matrix adaptation evolution strategy, evolutionary programming, particle swarm optimisation, genetic algorithm, and fireworks algorithm. Non-convex optimisation methods like non-convex projected gradient descent, generalized alternating minimization, Bayesian non-convex optimisation, and simulated annealing also have potential, especially in handling mutual coupling in non-uniformly spaced arrays. Covariance matrix adaptation evolution strategy was found to be optimal for array spacing and SLL minimization, while firework algorithm and genetic algorithm excelled in joint DOA and MCM estimation. Another optimisation method is used in [34] combining non-uniform elements spacing and combinatorial cyclic different sets (CDS). The spatial dimension of a 64-element linear microstrip full array is reduced to a 32-element linear sparse array using the proposed technique. results show that the sparse array's beamwidth resolution improved compared to the full array configuration, with only a minor increase in SLL degradation. Another development in the realm of sparse arrays is the concept of amplitude-density synthesis, as in [35]. This technique focuses on achieving optimal radiation patterns using non-uniformly spaced antenna elements. Two numerical procedures are proposed for this purpose. One is based on alternating optimisation of positions and amplitudes using closed-form convex projectors. The other is a domino-like sequential determination of the unknowns. The significance of amplitude-density synthesis lies in its ability to tailor the radiation pattern according to specific requirements, making it a versatile tool in the design of sparse arrays. Aperiodic arrays with amplitude–density tapering can outperform density tapered ones in several areas, including the extent of the controlled sidelobe region, the level of pseudograting lobes, and the variability of the interelement spacing. In-depth analysis of optimisation algorithms is outside the scope of this paper, however, [36] provides a very detailed report of the nature-inspired algorithms along with analysis and implementation techniques for the various types listed above along with others. Additionally, a visual summary of the references and designs discussed in this section is shown in Fig. 3.

References	Directivity considered	SLL considered	Mutual coupling considered	Mutual coupling compared	Beam steering considered	Algorithms considered	Algorithms compared
[15],	✗	✓	✓	✓	✗	✓	✗
[17]	✓	✓	✓	✗	✓	✓	✗
[18], [25], [32]	✗	✗	✓	✓	✗	✓	✓
[21]	✓	✓	✓	✓	✗	✓	✗
[22]	✓	✗	✓	✓	✗	✓	✗
[23], [26], [29], [30]	✗	✗	✓	✓	✗	✓	✗
[27]	✓	✓	✓	✓	✗	✓	✓
[28]	✗	✗	✓	✓	✓	✓	✗
[31]	✓	✓	✓	✓	✓	✓	✗
[33]	✓	✓	✓	✓	✓	✓	✓
[34]	✓	✓	✓	✗	✗	✓	✗
[35]	✓	✓	✗	✗	✗	✓	✓
This paper	✓	✓	✓	✓	✓	✓	✓

FIGURE 3. Reference summary table.

IV. ANALYSIS OF ARRAY DESIGN AND OPTIMISATION FOR MUTUAL COUPLING REDUCTION

This section discusses application-specific approaches targeting a specialized antenna array performance with a reduced mutual coupling in mind. The methods used in this section could be scaled and applied to various use cases for antenna arrays, such as base stations, handset antenna arrays, terrestrial, and non-terrestrial receivers etc. As previously mentioned, mutual coupling can be reduced through various means. When compared with ULAs mutual coupling can be reduced by either thinning the array by removing elements or sparsely placing the elements. This methodology works as it increases the average inter-element spacing, reducing the coupling between the elements. However, this alone is not enough, while this does reduce the mutual coupling, reducing the number of elements in the array through sparsity or thinning can also lead to a reduced gain in most instances given the same effective isotropic radiated power (EIRP). Previously mentioned techniques can be applied to optimise further the placements of these elements allowing the gain to be maintained or improved upon when compared with a uniform array.

In an investigation discussed further, optimisation was carried out for both the element position and element magnitude of the patch antennas within an array. Patch

Algorithm 1: Genetic Algorithm

Generate a random initial population, P_t
Set $t = 0$
while *Target criterion not met* **do**
  Select the best solutions for next generation
  Crossover, using crossover probability p_c
  Mutation, using mutation probability p_m
  Evaluate fitness of new solution, F^{t+1}
  if *Fitness has increased,* $F^{t+1} > F$ **then**
    Update fitness with new value, $F = F^{t+1}$
  end
  Iterate $t = t + 1$
end

Algorithm 2: Covariance Matrix Adaptation Evolution Strategy

Set sample rate, λ
Initialise CMA-ES parameters
$m, \sigma, C = I, p_\sigma = 0, p_c = 0$
while *Target criterion not met* **do**
  Evaluate fitness of solutions, F
  Sort solutions in terms of fitness
  Update mean, m
  Update evolution paths, p_σ, p_c
  Update covariance matrix, C
  Update step-size using evolution path lengths, σ
end

antennas were selected for this optimisation as they are more susceptible to the effects of mutual coupling than other arrays such as dipoles [22], so will benefit more from the mutual coupling reduction. These optimisations were carried out using various optimisation algorithms including: genetic algorithm (GA) [37], covariance matrix adaptation evolution strategy (CMA-ES) [38], particle swarm optimisation (PSO) [39], trust region framework (TRF) [40] Nelder-Mead simplex algorithm (NMSA) [41], interpolated quasi-Newton (IQN) [42] and classic Powell (CP) [43]. Detailed pseudo-codes for these algorithms are provided in Algorithms 1–7. Brief summaries of how each algorithm operates are also listed below. Simulations were carried out using the Finite-Difference Time-Domain (FDTD) solver within CST Microwave Studio. The frequency of the simulation was set at 28 GHz. Mesh cell properties were set as follows for each simulation:

- Maximum cell size of 15 cells per wavelength.
- 20 cells per maximum model box edge.
- 11 cells per maximum model box edge far from the model,
- Minimum cell size of ($\frac{1}{100}$ × maximum cell size near model).

The element positions were optimised within a range of the array that prevented overlapping of the elements, and the magnitudes were optimised within a range of 0.5 and 1. An example of the structure of the array and the possible element positions is shown in Fig. 4. Optimisation goals were set to improve the realised gain and reduce the SLL versus

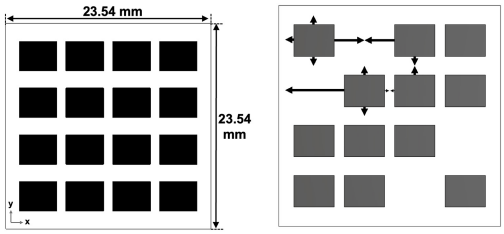

FIGURE 4. Diagram showing (a) 4 × 4 patch antenna array and dimensions, and (b) thinned 4 × 4 patch antenna array showing possible antenna element positioning.

Algorithm 3: Particle Swarm Optimisation

Generate swarm of particles of size, N
Initialise particle locations, x_i and velocities, v_i
Find the global best, g_b
while *Target criterion not met* **do**
  for *Each particle,* $i = 1, ..., N$ **do**
    Generate new particle velocities, v_i^{t+1}
    Generate new particle locations, x_i^{t+1}
    Evaluate objective function at new particle locations
    if *Current fitness is better than previous best,* $x_i^{t+1} > p_b$ **then**
      Update previous best with new value, $p_b = x_i^{t+1}$
    end
    if *Current fitness is better than global best,* $x_i^{t+1} > g_b$ **then**
      Update previous best with new value, $g_b = x_i^{t+1}$
    end
  end
  Iterate $t = t + 1$
end

Algorithm 4: Trust Region Framework

Choose a starting point, x_0
Evaluate the function at x_0
Initialise the trust region radius, r
while *Target criterion not met* **do**
  Calculate the search direction, d, using the trust region method
  Compute the step size, α, using a line search algorithm
  Update the point in the search space, $x = x + \alpha d$
  Evaluate the function at the new point, x
  Update the trust region radius, r, based on the success of the new solution
end

the full and thinned arrays to indirectly reduce the mutual coupling effects as supported by recent literature [44], [45]. Specifically, by optimising current excitation weights and inter-element spacing, one can achieve reduced sidelobe levels and null control, even without explicitly modelling mutual coupling in the optimisation process. In this study, while the mutual coupling was not modelled directly, the optimisation of gain and sidelobe level was leveraged to indirectly reduce its effects, providing a balanced approach to address the challenges posed by mutual coupling. Mutual

Algorithm 5: Nelder-Mead Simplex Algorithm

Initialise simplex using random values
Sort points in order of worst, second worst and best, x_w, x_m, x_b respectively
while *Target criterion not met* **do**
  Compute centroid, c
  Compute reflected, x_r
  if *Reflected is better than current best solution,* $f(x_r) > f(x_b)$ **then**
    Compute expanded, x_e Replace worst solution, x_w with better of reflected, x_r, or expanded, x_e
  end
  if *Reflected is better than second worst solution but worse than best solution,* $f(x_m) < f(x_r) < f(x_b)$ **then**
    Replace worst, x_w, with reflected, x_r
  end
  if *Reflected is worse than second worst solution,* $f(x_r) < f(x_m)$ **then**
    Compute contracted, x_c
  end
  if *Contracted is worse than worst solution,* $f(x_c) < f(x_w)$ **then**
    Shrink the search area
  else
    Replace worst, x_w, with contracted, x_c
  end
end

Algorithm 6: Quasi-Newton Method

Choose a starting point, x_0
Evaluate the function at x_0
Initialise the approximation of the Hessian matrix, H
while *Target criterion not met* **do**
  Calculate the search direction, d, using the conjugate gradient method
  Compute the step size, α, using a line search algorithm
  Update the point in the search space, $x = x + \alpha d$
  Evaluate the function at the new point, x
  Update the Hessian matrix approximation, H
end

Algorithm 7: Classic Powell

Choose a starting point, x_0
Evaluate the function at x_0
Initialise a direction vector, d
while *Target criterion not met* **do**
  Compute the step size, α, using a line search algorithm
  Update the point in the search space, $x = x + \alpha d$
  Evaluate the function at the new point, x
  Update the direction vector, d
end

coupling values have been assessed both before and after the optimisation to determine the effects.

A generalized mathematical model for mutual coupling is provided. Similar models have been used in sparse and thinned array papers of a related nature [27], [46], [47], [48], [49], [50]. Mutual coupling, especially pronounced when antennas are closely spaced, can be represented in the received signal vector as:

$$x(t) = CAs(t) + n(t) \tag{1}$$

where:

- $x(t)$ is the received signal vector.
- C is the $N \times N$ mutual coupling matrix.
- A is the array manifold matrix.
- $s(t)$ is the signal waveform vector.
- $n(t)$ is the noise.

In scenarios devoid of mutual coupling, C simplifies to an identity matrix. For linear arrays, such as ULAs, the mutual coupling matrix C can be approximated as a B-banded symmetric Toeplitz matrix, defined by:

$$C_{ij} = \begin{cases} c|i-j| & \text{if } |i-j| \leq B \\ 0 & \text{otherwise} \end{cases} \tag{2}$$

where:

- i, j are the positions of the elements.
- $c_0, c_1, \ldots, c_B$ are the coupling coefficients, with $c_0 = 1$ and the magnitudes of the coefficients decreasing as their indices increase.
- The magnitudes of the coupling coefficients are typically inversely proportional to the separation between the elements.

It is crucial to highlight that in this specific study, the simulated coupling metrics between individual antenna elements was assessed. This was done by utilizing an EM Solver, CST Studio, specifically the transient solver, to compute the coupling values, ensuring precise results tailored to the specific array configurations. The average and peak mutual coupling values displayed below are calculated by taking the coupling values between the individual antenna elements that are in the nearest proximity to each other.

It should be noted that this study has adhered to a consistent strategy across all algorithmic evaluations. The focus is on a uniform approach, transitioning from a consistent thinned array to its optimised counterpart. This ensures that analysis is centred on the effectiveness of the algorithms used, limiting possible strategic variations. Such an approach allows for an unbiased comparison of each algorithm within a defined optimisation framework. While the choice of algorithm is pivotal, it is paramount to recognize the importance of a consistent strategy. This study highlights the comparative merits of various algorithms, all evaluated under this unified strategy.

Genetic Algorithm: A stochastic optimisation technique that is based on the principles of natural selection and genetics. It starts with a random population of solutions and iteratively applies genetic operators such as selection, crossover and mutation to the population in order to evolve it towards better solutions.

Covariance Matrix Adaptation Evolution Strategy: A stochastic optimisation algorithm that is particularly well-suited for high-dimensional optimisation problems. It adapts the step-size and search direction using the covariance matrix of the population.

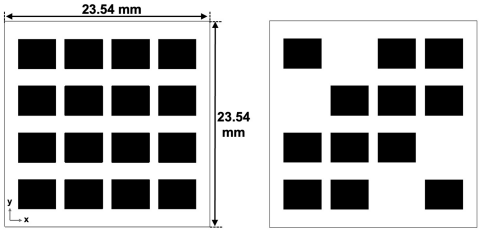

FIGURE 5. Diagram showing (a) 4 × 4 patch antenna array and dimensions, and (b) thinned 4 × 4 patch antenna array.

Particle Swarm Optimisation: An population-based optimisation algorithm that simulates the social behavior of birds or insects in order to find an optimal solution. It uses the concept of a swarm of particles that move in the search space, where each particle is guided by its own best position and the best position of the entire swarm.

Trust Region Framework: An optimisation method that is based on the concept of trust regions. It iteratively improves an approximation of the solution by constructing a quadratic model of the objective function within a trust region and solving the resulting trust-region sub-problem to find a new approximation.

Nelder-Mead Simplex Algorithm: An optimisation method that is based on the simplex method. It starts with a simplex of $n + 1$ points in n-dimensional space and iteratively reflects, expands, contracts, or shrinks the simplex in order to converge to the optimal solution.

Quasi-Newton Method: An optimisation method that uses an approximation of the Hessian matrix to improve the efficiency of the optimisation process. It aims to find a fast convergence rate by iteratively updating an approximation of the Hessian matrix and using it to calculate the search direction.

Classic Powell: An optimisation method that is based on the concept of a downhill simplex method. It is a direct search method that does not require the gradient of the function, it starts with a simplex and tries to improve the current point by moving along the edges of the simplex. If the movement is not improving the solution it contracts the simplex and repeats the process.

A. 4 × 4 ARRAY MUTUAL COUPLING REDUCTION

Experimentation has been carried out to demonstrate the effects of sparse array development and then the application of various optimisation algorithms to further improve the realised gain and side-lobe level (SLL) of the sparse array. The antenna selected for this experimentation is a coax feed microstrip patch antenna, operating at 28 GHz. The analysis was first carried out on a 4×4 patch antenna array operating at 28 GHz, which can be seen in Fig. 5 (a). This array has a realised gain of 15.5 dBi and a SLL of -13.5 dBi. The array was thinned by removing 4 antenna elements, leaving only 12 elements, as shown in Fig. 5 (b). Removal of this element led to a reduced realised gain of 15.3 dBi and a SLL of -13.9 dBi.

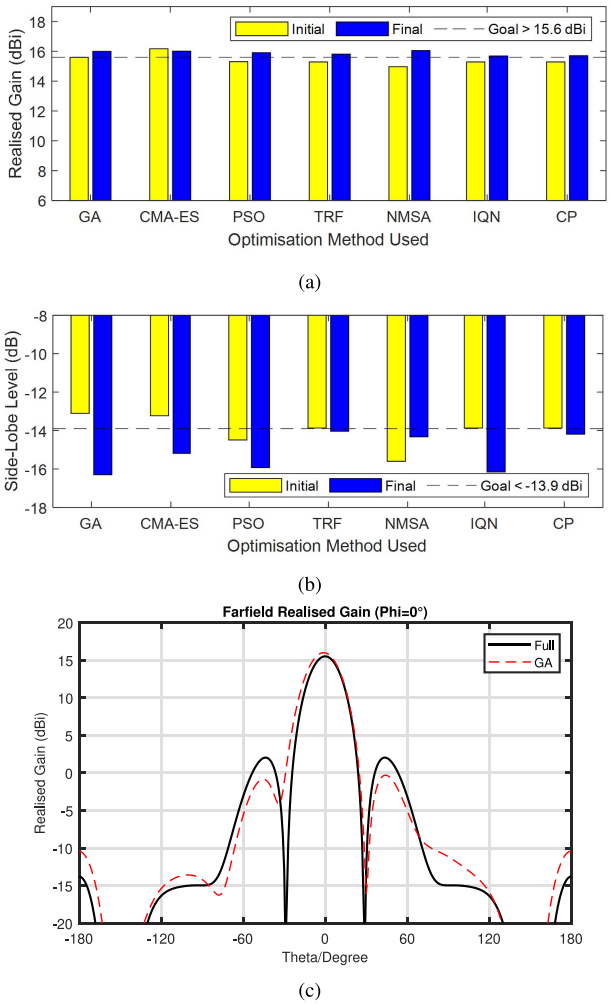

FIGURE 6. Optimisation comparisons of 4 × 4 array for (a) Realised gain. (b) SLL. (c) Radiation pattern.

Specifically, the realised gain goal was set as > 15.6 dBi, and the SLL goal was set as < -13.9 dBi. Algorithms stopped when these targets were achieved. Results for both the realised gain and the SLL can be seen in Fig. 6 (a) and (b). Results show that NMSA achieved the highest final realised gain value of 16.1 dBi, while GA achieved the lowest SLL value of -16.3 dBi. An comparison of the radiation pattern for the full 4×4 array with the GA configuration can be seen in Fig. 6 (c).

The next area of assessment is the number of runs taken to achieve the goals set out for the optimisation tasks above. Each run consists of a complete solver run with updated optimisation parameters for magnitude and element positions, therefore, each run will complete in a consistent time frame dependent upon the computational power available to the user. It should be noted for the number of runs, that only solver runs were considered for the results as these affect the run times for the simulations; interpolated

TABLE 1. Run comparison of 4 × 4 array for different optimisation algorithms.

Optimisation Method	GA	CMA-ES	PSO	TRF	NMSA	IQN	CP
Number of Runs	30	2	18	39	3	269	13

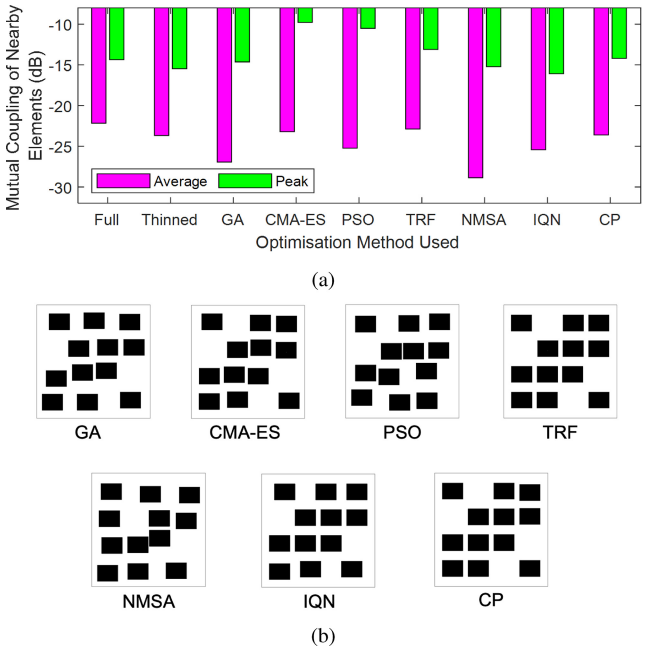

FIGURE 7. (a) Mutual coupling comparisons of 4 × 4 array for different optimisation algorithms. (b) Final element positions of 4 × 4 array for different optimisation algorithms.

evaluations, such as in IQN were not counted for these results. Additionally, for algorithms that failed to meet the optimisation targets, run counts are given for the number of runs taken before the solver stopped and returned the best-found solution. Note that one can have a direct translation of the number of runs to an accurate computational load for each algorithm, however, this is out of the scope of this study. All optimisation algorithms were successful in meeting the targets, with CMA-ES being the most efficient in terms of the number of runs required as seen in Table 1.

Mutual coupling, the most important parameter, was analyzed by taking the coupling values of the nearby elements at 28 GHz and calculating both the average and peak values for the final array configuration for each algorithm. In terms of average mutual coupling values, NMSA had the best performance with the lowest value of −28.9 dB, while CMA-ES had the worst performance with a peak mutual coupling value of −9.79 dB, as shown in Fig. 7 (a). It should be noted that in the mutual coupling plots presented, the mutual coupling of nearby elements is depicted in negative dB values. A larger magnitude on the plot indicates a lower mutual coupling. While there are instances of higher peak mutual coupling values in the optimised sparse arrays, the method generally results in a reduced average mutual coupling due to increased average inter-element spacing. The element positions of the 4 × 4 array with the various optimisation algorithms can be seen in Fig. 7 (b). Some elements were spaced considerably close, which resulted in high peak mutual coupling values in CMA-ES and PSO. Final antenna placement configurations for the arrays for each algorithm show that each algorithm can provide a different optimised solution depending on the problem set.

B. 4 × 4 ARRAY WITH BEAM STEERING

Beam steering capability is a crucial aspect of array optimisation, but it is not guaranteed that a sparse array resulting from optimisation will possess the same steering ability as a full array within the required field-of-view (FoV). Sparse arrays have limitations compared to full arrays, as they generate weaker beams when steered away from the boresight and have a restricted steering range [51]. However, sparse arrays can still produce beams with similar width to full arrays and offer reasonable performance for beam steering applications while reducing hardware requirements [52]. Additional insight into this aspect is provided by the analytical expression for directivity in the context of wide scanning characteristics of sparse phased arrays [53]. This analytical approach offers a deeper understanding of the beam steering capabilities, emphasizing the performance of sparse arrays in wide scanning applications. This paper offers a tool for predicting the precise locations of blind spots in the desired scan volume due to the chosen array geometry, and also delves into the wide scan characteristics of periodic sparse phased array antennas using the proposed expressions. This section presents a novel analysis considering different array types and non-uniform element positioning. Various optimisation algorithms are employed to understand their performance in different scenarios, including how a previously optimised array performs with beam steering and improving the performance of a fixed beam sparse array steered from boresight.

To investigate this, a non-ideal 4 × 4 array is optimised for multiple beam configurations. Beam steering is achieved through phase shifting, where each element undergoes a phase step (Φ). Φ represents the phase difference between neighbouring elements. For example, a Φ value of 30° indicates a phase of 0° at the first element, 30° at the second element, 60° at the third element, and so on. It is important to note that Φ does not directly indicate the desired beam direction when steering. Φ is increased from 0° to 30° in 10° intervals, and the realized gain and SLL values are recorded for each array to evaluate their performance. While the optimisation algorithms result in different element positions for the sparse array, the phase of each element remains consistent across arrays, regardless of position. This slight variation in beam angle allows for testing the resilience of the optimised sparse arrays to beam steering.

Realised gain comparisons can be seen in Fig. 8 (a). The general trend is the same for each array configuration, with a decrease in the realised gain as Φ is increased. The full 4 × 4 array had the lowest decrease in realised gain between Φ values of 0° and 30°, with a decrease

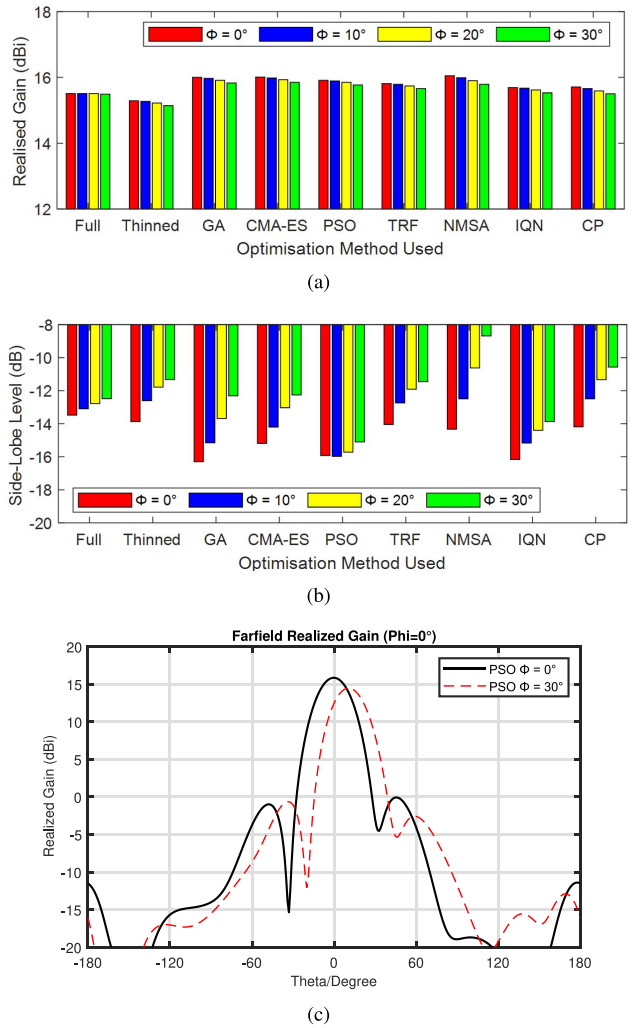

FIGURE 8. Beam scanning comparison of optimised 4 × 4 array configurations for (a) Realised gain. (b) SLL. (c) Radiation pattern.

of 0.13%. Out of the optimised configurations, PSO had the lowest reduction in gain at 0.88% while NMSA had the largest reduction of 1.6%. SLL comparisons can be seen in Fig. 8 (b). The full array had an increase to SLL of 7.42%. In terms of optimised placements PSO had the smallest increase at 5.21%, while NMSA had the largest increase at 39.4%. Radiation patterns with the application of beam steering for the PSO array configuration are shown in Fig. 8 (c) (Φ values correspond to phase step values applied to the array.) A summary table of the 4×4 optimised array configurations, is shown in Table 2. This table contains a tabulated version of all the data presented in this section.

The investigation was also carried out when beam steering is applied to the 4×4 array to see how the optimisation algorithms alter the element configurations. Beam steering was carried out on the full 4×4 array to determine the realised gain and SLL values, along with mutual coupling performance. This was done using phase shift

TABLE 2. Optimisation summary of 4 × 4 array.

Array	Peak Gain (dBi)	Avg. SLL (dB)	Inter-element Spacing (mm)		Mutual Coupling (dB)		No. of runs	Beam Steering Variation (Φ0 − 30°) (% Decrease)	
			Min.	Max.	Avg.	Peak		Gain	SLL
Full	15.51	-13.48	5.35	5.35	-22.17	-14.36	-	0.13	7.42
Thinned	15.29	-13.87	5.35	10.70	-23.68	-15.48	-	0.98	18.39
GA	16.0	-16.3	4.96	8.95	-26.94	-14.64	30	1.06	24.48
CMA-ES	16.01	-15.19	4.84	10.69	-23.21	-9.79	2	1.00	19.29
PSO	15.91	-15.93	4.61	9.01	-25.24	-10.52	18	0.88	5.21
TRF	15.81	-14.04	5.25	10.79	-22.88	-13.11	39	0.95	18.44
NMSA	16.05	-14.33	4.50	10.35	-28.87	-15.22	3	1.62	39.43
IQN	15.69	-16.16	5.35	8.57	-25.43	-16.09	269	1.02	14.17
CP	15.71	-14.19	5.35	10.70	-23.62	-14.20	13	1.34	25.51

TABLE 3. Run comparison of 4 × 4 array, with beam steering, for different optimisation algorithms.

Optimisation Method	GA	CMA-ES	PSO	TRF	NMSA	IQN	CP
Number of Runs	5	10	2	39	1	176	43

values increasing in steps of 30° for each consecutive element. Realised gain for the full array was calculated as 15.5 dBi and the SLL value was −12.5 dBi. Then in a similar fashion to the 4×4 array in the previous section, elements were removed to form a thinned array. Phase shift values remained constant for the remaining elements. Full and thinned array configurations are the same as shown in Fig. 5 in the previous section. Optimisation was carried out, similar to the previous sections, while keeping phase values constant. Targets for the realised gain and SLL were set as >15.5 dBi and < −12.5 dBi respectively. As shown in Fig. 9 (a), only TRF failed to meet the realised gain target. GA was the top performer with a realised gain of 16.0 dBi. Similarly, in Fig. 9 (b), only TRF failed to meet the SLL target, with IQN achieving the lowest SLL value at −15.0 dBi. Radiation patterns for beam steering with a Φ value of 30° are shown in Fig. 9 (c) for the full 4×4 array along with the PSO configuration.

In terms of efficiency, NMSA had the least number of runs as seen in Table 3, only taking one run to meet the targets, while IQN took the most runs out of the algorithms that successfully met the targets, taking 176 runs. PSO is notably efficient also, only taking 2 runs to meet the optimisation targets.

The results for average mutual coupling values are shown in Fig. 10 (a), NMSA had the best performance with a value of −28.5 dB, while CMA-ES had the worst performance with a value of −22.8 dB. In terms of peak mutual coupling, GA had the lowest peak value at −18.41 dB, while PSO had the highest at −11.3 dB.

Finally, the element position configurations for each algorithm can be seen in Fig. 10 (b). It is clear that the element placement configurations have changed significantly from the previous section when no phase shift was applied to the elements. This implies that optimisations are only applicable for specific scenarios. When variables such as phase shift are changed, the optimal solution will also change. Once again, a tabulated summary can be seen in Table 4 for the updated 4×4 array beam steering configurations.

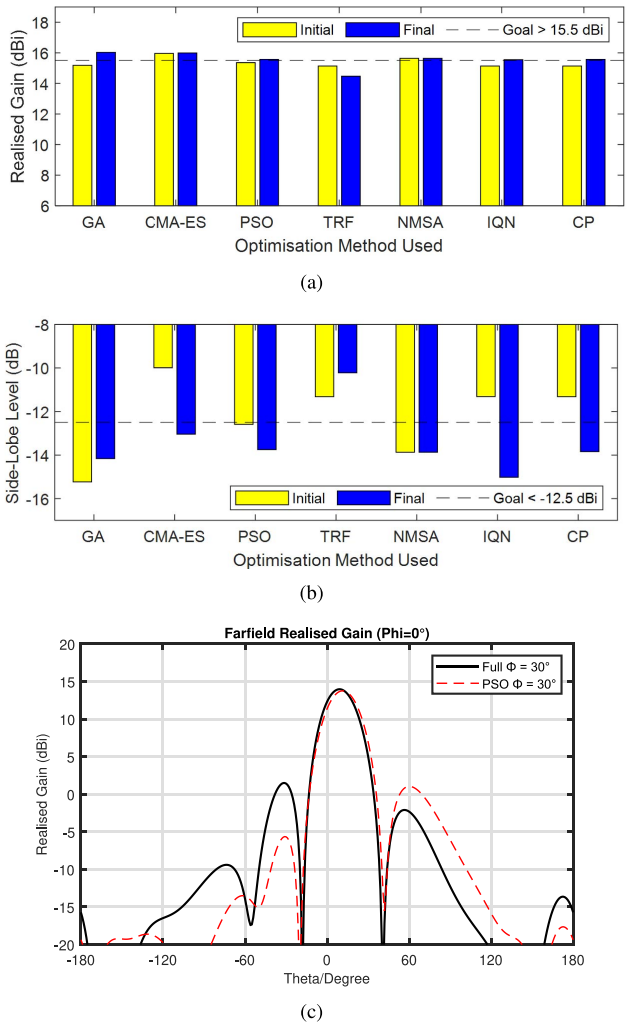

FIGURE 9. Optimisation comparisons of 4 × 4 array, with beam steering, for (a) Realised gain. (b) SLL. (c) Radiation pattern.

TABLE 4. Optimisation summary of 4 × 4 array, with beam steering.

Array	Peak Gain (dB)	Avg. SLL (dB)	Inter-element Spacing (mm)		Mutual Coupling (dB)		No. of runs
			Min.	Max.	Avg.	Peak	
Full	15.49	-12.48	5.35	5.35	-22.17	-14.35	-
Thinned	15.14	-11.32	5.35	10.70	-23.74	-15.48	-
GA	15.18	-14.16	4.32	8.55	-27.15	-18.41	5
CMA-ES	15.96	-13.04	5.01	10.75	-22.84	-11.82	10
PSO	15.36	-13.75	5.11	9.28	-25.98	-11.31	2
TRF	15.14	-10.22	5.41	10.70	-26.40	-13.61	39
NMSA	15.64	-13.87	5.11	8.21	-28.48	-16.67	1
IQN	15.14	-15.02	4.83	9.52	-27.71	-13.84	176
CP	15.14	-13.84	5.35	10.70	-23.32	-13.49	43

C. LINEAR ARRAY MUTUAL COUPLING REDUCTION

A similar analysis as in the previous section, has been carried out on a linear array with a patch antenna design and a 16×1 element configuration with a $\lambda/2$ spacing, shown in Fig. 11 (a). The thinned array (Fig. 11 (b)) was optimised using similar methods, with targets set as a realised gain of $>$ 15.9 dBi and SLL of < -13.5 dBi. The element magnitude and position along the x-plane were varied during the optimisation. Radiation patterns for the full array and the NMSA configuration are shown in Fig. 12 (c).

The results show that PSO and NMSA provide the best performance in terms of realised gain and SLL respectively, shown in Fig. 12, while NMSA once again provides the best average mutual coupling performance, with IQN providing the lowest peak value, shown in Fig. 13 (a). NMSA takes the shortest time to achieve the targets, while CMA-ES takes the longest time. Element positions for these optimised array configurations can be seen in Fig. 13 (b).

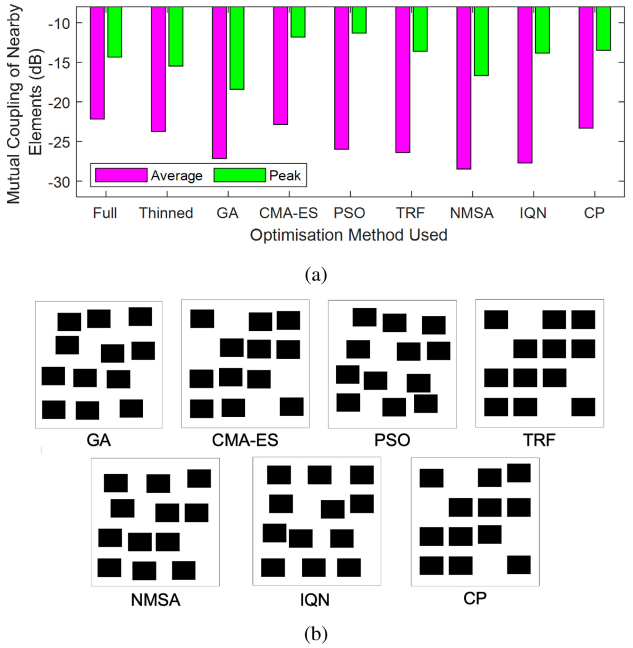

FIGURE 10. (a) Mutual coupling comparisons of 4 × 4 array, with beam steering, for different optimisation algorithms. (b) Final element positions of 4 × 4 array, with beam steering, for different optimisation algorithms.

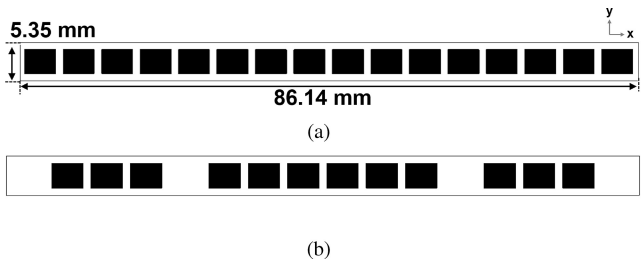

FIGURE 11. Diagram showing (a) 16 × 1 patch antenna array and dimensions, and (b) thinned 16 × 1 patch antenna array.

TABLE 5. Run comparison of 16 × 1 array for different optimisation algorithms.

Optimisation Method	GA	CMA-ES	PSO	TRF	NMSA	IQN	CP
Number of Runs	26	174	3	105	1	110	23

D. LINEAR ARRAY WITH BEAM STEERING

Similar to the 4×4 array, beam steering is applied to the linear array to determine how the optimised placements perform when the beam direction is changed. Beam scanning performance for each array configuration can be seen in

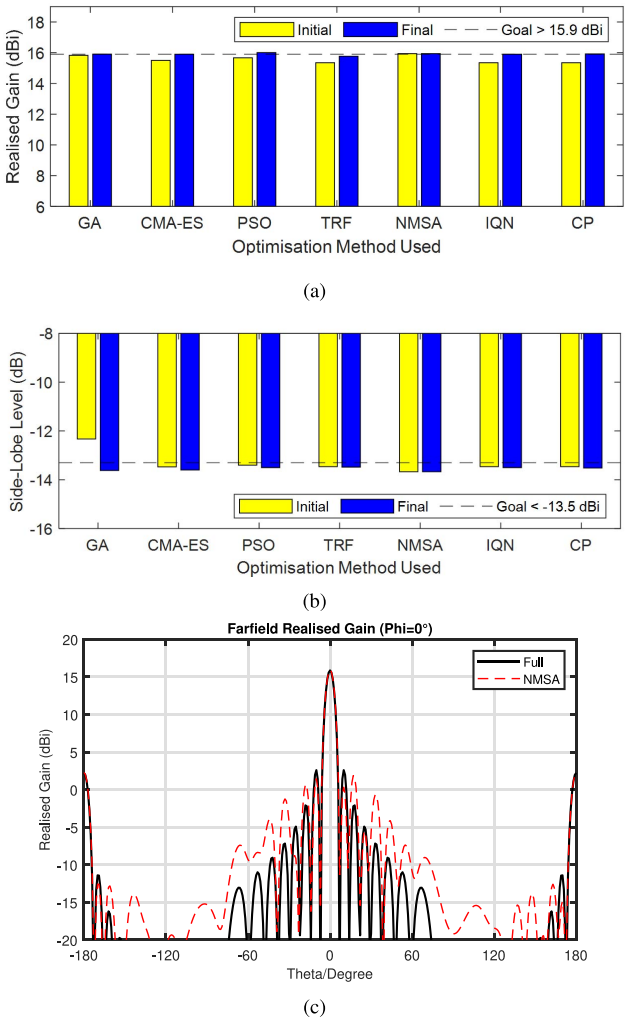

FIGURE 12. Optimisation comparisons of 16 × 1 array for (a) Realised gain. (b) SLL. (c) Radiation pattern.

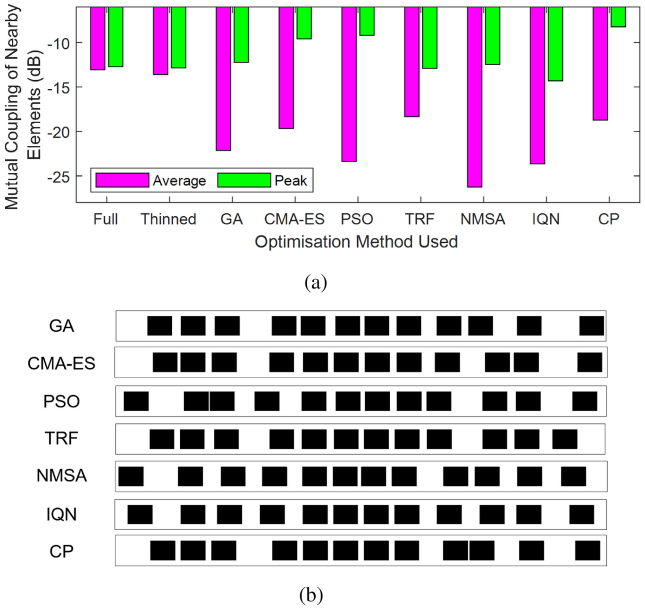

FIGURE 13. (a) Mutual coupling comparisons of 16 × 1 array for different optimisation algorithms. (b) Final element positions of 16 × 1 array for different optimisation algorithms.

TABLE 6. Optimisation summary of linear 16 × 1 array.

Array	Peak Gain (dBi)	Avg. SLL (dB)	Inter-element Spacing (mm)		Mutual Coupling (dB)		No. of runs	Beam Steering Variation ($\Phi 0 - 30°$) (% Decrease)	
			Min.	Max.	Avg.	Peak		Gain	SLL
Full	15.85	-13.27	5.35	5.35	-13.07	-12.72	-	0.25	0.15
Thinned	15.35	-13.46	5.35	10.70	-13.61	-12.86	-	0.78	4.53
GA	15.91	-13.62	5.09	10.97	-22.14	-12.24	26	1.57	6.46
CMA-ES	15.9	-13.6	4.83	11.09	-19.67	-9.58	174	1.01	1.76
PSO	16.01	-13.5	4.55	10.52	-23.37	-9.20	3	1.06	0.74
TRF	15.77	-13.48	5.31	9.76	-18.34	-12.90	105	0.63	3.04
NMSA	15.94	-13.67	4.96	10.39	-26.25	-12.47	1	1.25	15.29
IQN	15.9	-13.5	5.35	9.26	-23.65	-14.31	110	0.94	0.96
CP	15.92	-13.52	4.62	10.70	-18.72	-8.23	23	1.95	12.72

TABLE 7. Run comparison of 16 × 1 array, with beam steering, for different optimisation algorithms.

Optimisation Method	GA	CMA-ES	PSO	TRF	NMSA	IQN	CP
Number of Runs	66	233	63	79	97	319	64

Fig. 14(c). All the optimised array configurations follow the same general trend of reduction in gain values as the phase shift is increased (Fig. 14(c)). The full array had an overall decrease in realised gain of 0.25% between Φ values of 0° and 30°. TRF had the lowest gain reduction from beam steering out of the optimised array configurations. However, TRF failed to meet the optimisation targets set out previously. For configurations that achieved the targets, PSO provides the highest gain value for each Φ value with an overall decrease of 1.06%. CP has the highest overall decrease out of the configurations at 1.95%. In terms of SLL performance the full array has an overall decrease of 0.15%. Of optimised configurations, PSO has the smallest increase in SLL when beam steering is applied with an overall increase of 0.74%. NMSA has the largest increase with 15.3%. Radiation patterns for the PSO configuration with the application of beam steering are shown in Fig. 14(c). Additionally, a summary of the optimised 16×1 linear array configurations is tabulated and shown in Table 6.

Similar to the 4×4 array, optimisation has again been carried out for different beam steering configurations. Using a Φ value of 30°, the magnitude and placement of the elements can be optimised. The realised gain results for the beam steering scenario are illustrated in Fig. 15 (a). TRF did not meet the target realised gain of 15.9 dBi, however, NMSA had the most promising result with a realised gain of 16.0 dBi. As shown in Fig. 15 (b), TRF was again unsuccessful in meeting the SLL target, whereas, NMSA came up with the best configuration with the lowest SLL of −13.5 dBi. Optimised beam steering configurations can be seen for the full array and the PSO configuration, shown in Fig. 15 (c). The number of runs taken by each algorithm is detailed in Table 7. PSO was the most efficient with only 63 runs, while IQN required the most with 319 runs.

We also evaluated the mutual coupling performance of the array. The full array had an average mutual coupling

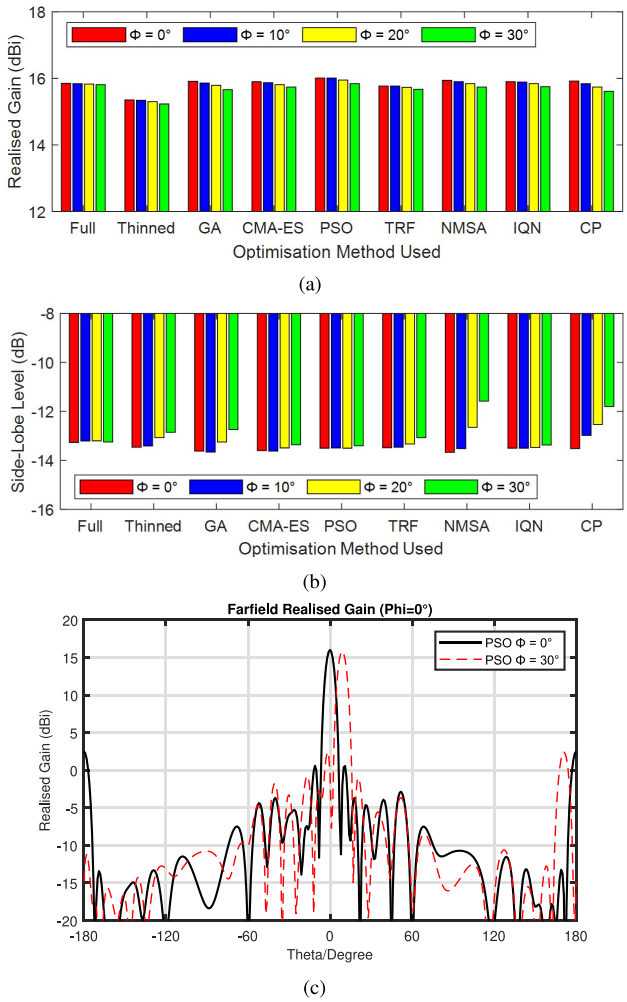

FIGURE 14. Beam scanning comparison of optimised 16 × 1 array configurations for (a) Realised gain. (b) SLL. (c) Radiation pattern.

TABLE 8. Optimisation summary of linear 16 × 1 array, with beam steering.

Array	Peak Gain (dBi)	Avg. SLL (dB)	Inter-element Spacing (mm)		Mutual Coupling (dB)		No. of runs
			Min.	Max.	Avg.	Peak	
Full	15.49	-12.48	5.35	5.35	-22.17	-14.35	-
Thinned	15.14	-11.32	5.35	10.70	-23.74	-15.48	-
GA	15.18	-14.16	4.32	8.55	-27.15	-18.41	5
CMA-ES	15.96	-13.04	5.01	10.75	-22.84	-11.82	10
PSO	15.36	-13.75	5.11	9.28	-25.98	-11.31	2
TRF	15.14	-10.22	5.41	10.70	-26.40	-13.61	39
NMSA	15.64	-13.87	5.11	8.21	-28.48	-16.67	1
IQN	15.14	-15.02	4.83	9.52	-27.71	-13.84	176
CP	15.14	-13.84	5.35	10.70	-23.32	-13.49	43

value of −13.1 dB and a peak mutual coupling value of −12.72 dB. Out of the optimisation algorithms, NMSA had the best results with the lowest average mutual coupling value of −25.6 dB, as seen in Fig. 16 (a). NMSA also had the lowest peak value at −15.5 dB. CMA-ES had the highest peak value at −7.96 dB. The final element positions for this beam steering configuration are shown in Fig. 16 (b). Again, a summary table of the data for the optimised 16 × 1 linear array configurations, with beam steering, is shown in Table 8.

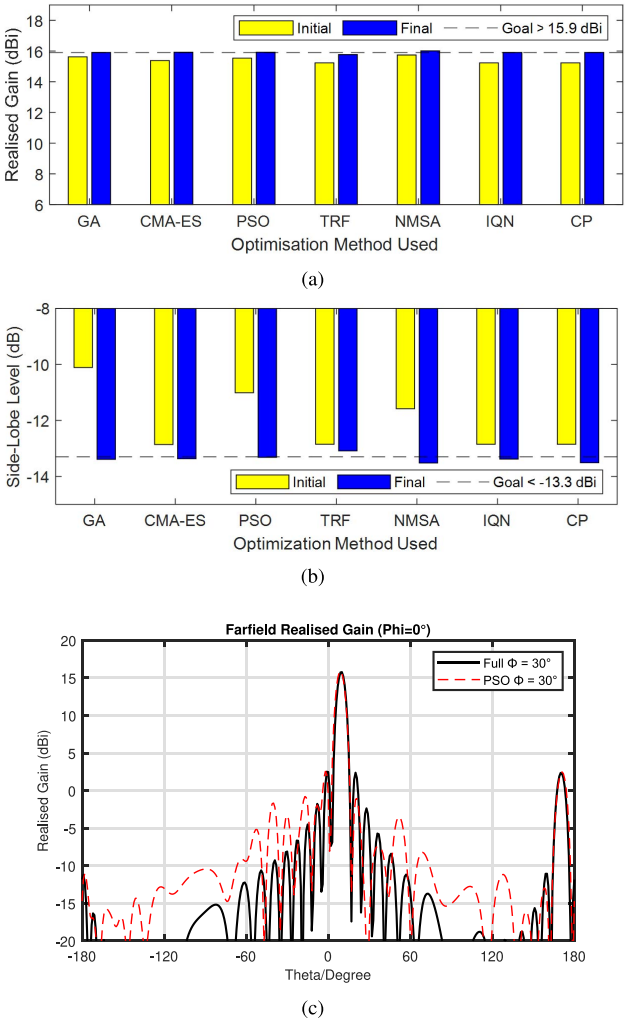

FIGURE 15. Optimisation comparisons of 16 × 1 array, with beam steering, for (a) Realised gain. (b) SLL. (c) Radiation pattern.

V. DISCUSSION

Optimisation of the antenna arrays allows the optimised array configurations to match or exceed the realised gain and SLL performance of the array configuration when it is completely filled with antenna elements. This allows for hardware reduction within the arrays to reduce the hardware costs and overall power consumption, making the arrays more efficient. As showcased, various algorithms are capable of optimising the array configuration successfully, however after the various simulations were carried out, it is clear that some algorithms are better suited to this type of optimisation problem.

PSO provides consistent results for the majority of the array configurations. Achieving all the optimisation targets for every array configuration in a reasonable number of solver runs. Additionally PSO consistently manages to achieve an average mutual coupling value lower than that of the full array for every array configuration. Other algorithms also achieve this, such as NMSA which on multiple

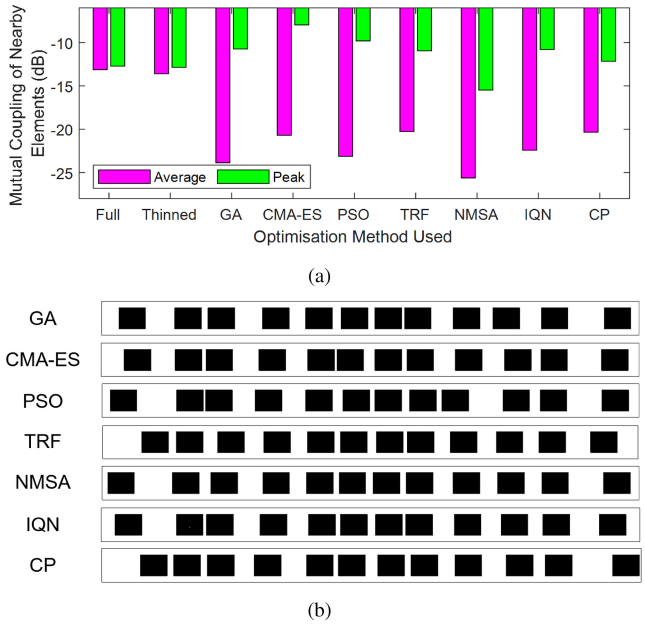

FIGURE 16. Optimisation comparisons of 16 × 1 array, with beam steering, for (a) Mutual coupling. (b) Final element positions.

Phase Step Value Φ (°)	4×4 Full Array		4×4 PSO Optimised Array	
	Realised Gain (dBi)	SLL (dB)	Realised Gain (dBi)	SLL (dB)
30	15.5	-12.5	15.8	-14.7
60	15.3	-11.5	15.4	-12.8
90	14.9	-10.7	14.4	-11.0
120	14.5	-9.60	12.8	-7.00
150	13.6	-7.60	9.97	-2.60
180	11.1	-4.80	7.52	-0.50

FIGURE 17. Comparison of beam scanning range for full 4×4 array and PSO optimised array.

occasions provided the best mutual coupling performance along with converging the fastest. However, NMSA had significant performance reductions for the optimised placements when beam steering, producing the largest reduction in realised gain for the optimised 4 × 4 array, along with the largest increase in SLL for both the optimised 4 × 4 and 16 × 1 arrays with beam steering. PSO however, produced an optimised solution in both cases that was more resilient to performance reductions while beam steering, providing realised gain and SLL values that remained better than the full array for both the optimised 4 × 4 and 16 × 1 arrays. NMSA seems to be suitable for optimisation of array configurations for fixed beam applications.

Beam scanning performance can also be assessed more rigorously. Juxtaposing the beam scanning performance of a full 4 × 4 array with its PSO optimised counterpart as seen in Fig. 17. Results revealed intriguing nuances in their respective performances. For Φ values up to 60°, the PSO configuration exhibited superior performance compared to the full array. Specifically, the optimised array showcased a heightened gain and a diminished SLL, underscoring its efficacy in scenarios demanding limited beam scanning. This is a testament to the optimisation process, which, while focusing on specific performance metrics, inadvertently enhanced the array's scanning capabilities within this range. However, it is worth noting that beyond 90° Φ value, the gain of the optimised array begins to deteriorate, and the SLL increases. This observation underscores the inherent trade-offs in antenna array design. While the optimised array shows improved performance in limited scanning scenarios, its performance wanes when extensive scanning is required. For systems and applications where extensive beam scanning is not imperative, the PSO configuration offers a compelling alternative, marrying efficiency with performance. Its ability to deliver superior results within a specific scanning range accentuates the potential of optimisation techniques in tailoring antenna arrays for niche applications.

Previous study [33], as mentioned in the paper, suggested that CMA-ES provided the best performance for sparse placement of antenna elements, as stated this study made use of nature-inspired optimisation algorithms, providing crossover with our own simulations, using GA, CMA-ES and PSO. The differentiating factor in this conclusion is likely the use of dipole antennas in the previous study as opposed to patch antennas in this work. This conclusion is backed by the no-free-lunch theorem that suggests that no one algorithm is superior for all optimisation problems, and that changing an optimisation problem can lead to an entirely different optimisation algorithm being more suitable for that given problem [54].

It may also be possible to further improve the performance of these algorithms through the use of tuning, tuning essentially allows for the optimisation of the given algorithms for a specific problem, producing optimal parameter sets that allow for the best performance. This tuning however is problem specific and will change depending upon the optimisation problem [36]. Tuning was outside the scope of this study and further research could be carried out into these tuning methods in attempts to further improve the performance of the successful algorithms shown in this paper. In addition to this, further work may be carried out into the assessment of optimisation algorithms for sparse array optimisation and mutual coupling reduction. It has been shown that through array performance optimisation that sparse arrays can improve upon the performance of a uniform array, additionally mutual coupling performance can also improve during this optimisation due to the increased average inter-element spacing as seen in the simulations. The majority of sparse array papers that report reduced mutual coupling are purely based upon this increase in inter-element spacing. However, other methods such as the optimisation of the MCM allow for significantly better mutual coupling performance. Further research can be carried out to a greater extent focusing on the optimisation algorithms and how they operate to determine what makes specific algorithms better suited for certain types of array optimisation, including both element placement and processing of the MCM. With this knowledge it could be possible to design a more

complete framework to ensure the optimal mutual coupling performance for a given antenna array. In parallel to this, additional study can be carried out investigating potential hardware improvements to the work carried out here. More specifically combining this work with the emerging movable antenna technology, which presents a transformative avenue for enhancing the adaptability and performance of communication systems. Under different scenarios, the flexible antenna movement can equivalently yield different array geometries such that the adaptability of sparse arrays can be further enhanced. Such designs have been showcased in previous studies [55], [56], [57] and are more recently discussed in [58], [59]. Reconfigurable antennas possess the ability to modify their polarisation, operating frequency, or far-field pattern in response to changing system parameters. This adaptability is achieved through differing mechanisms, from mechanically movable parts to advanced semiconductor-component and tuneable-material technologies. For instance, the use of RF switches allows for dynamic control over the current path on a reconfigurable antenna, enabling alterations in the antenna's radiation properties. Furthermore, large-scale implementations demonstrate the feasibility of physically moving antenna elements to achieve desired configurations.

It is also worthwhile mentioning the similarity of the linear array optimisation to dense array configurations. It is evident that the optimised sparse array exhibits a dense central portion. This observation is crucial as it underscores an inherent characteristic of our optimisation process. The primary aim of our study was to demonstrate that, through non-uniform element placement, a sparse array can achieve performance metrics that are comparable to, or even surpass, those of a full array. Given the one-dimensional spacing constraint within the linear array, where elements can only move horizontally, the optimisation often converges towards solutions that bear a resemblance to dense array structures, the concept of which is shown in Fig. 18 (e). This dense central portion of our optimised sparse array would likely exhibit performance characteristics, especially in terms of mutual coupling, akin to those of a dense array. Such a resemblance is not coincidental but rather an outcome of the optimisation process aiming to satisfy specific targets. It is worth noting that while our optimisation seeks to demonstrate the potential of sparse arrays, the resulting structures often mirror the performance of their dense counterparts.

Several designs from recent years [60], [61] have showcased improved performance. These findings provide a broader context to our results and show the potential of sparse arrays in mimicking the performance of dense arrays. In future research, it would be beneficial to delve deeper into this similarity, exploring the nuances of sparse and dense arrays and their respective performance metrics in various scenarios.

In terms of possible applications of the methodologies shown in this paper, the optimisations used can be applied to

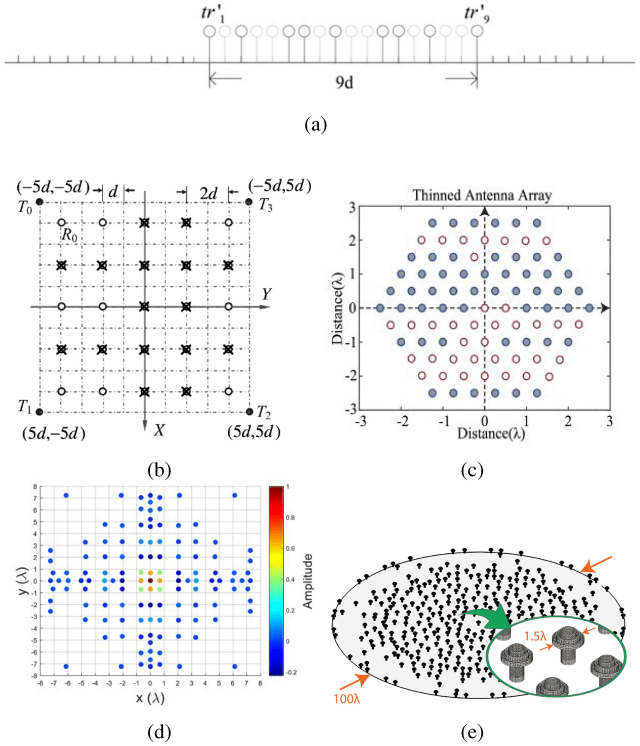

FIGURE 18. Sparse array configurations for (a) 2D MIMO radar imaging [62], (b) 3D MIMO radar imaging [63], (c) adaptive beamforming [64]. (d) Sparse array configuration with minimum spacing constraint [65]. (e) A synthesized dense array comprising of pipe horn antennas [60].

various antenna designs in an effort to reduce the number of antenna elements and maintain performance, all the while, reducing the overall mutual coupling of the antenna array with an increased average inter-element spacing. The designs shown in Fig. 18 (a) - (d) all make use of sparse array techniques to improve upon standard full array designs used for the same application. The arrays however could be described as quite uniform in their sparsity, with these examples displaying considerable symmetrical properties in their designs. An array layout with a less uniform configuration, as shown in this work, will allow for more possible optimised configurations for the given optimisation algorithm, which in turn, may allow for an increase in the average inter-element spacing leading to a reduction in the mutual coupling, while still sustaining the main benefits of the sparse array design.

VI. CONCLUSION

This paper has provided a summary of the state of the art around mutual coupling reduction within sparse arrays. It has been shown that there are a number of varying sparse array designs that report having reduced mutual coupling, due to an increased inter-element spacing. It has also been shown that there are other possible methods of mutual coupling reduction that can be used such as, MCM estimation and processing, and also the use of optimisation algorithms to optimise the antenna arrays. Simulations results have been

shown for various array configurations, demonstrating that optimisation of the antenna arrays can lead to reduced hardware costs by means of reducing the number of elements in the array. Furthermore it has been shown that these optimisation methods can further improve the performance over that of a full array. It is shown that through these optimisations mutual coupling can also be reduced. PSO is shown to be the most suitable optimisation algorithm for the tested sparse array structures, 4×4 and 16×1, due to the ability to efficiently improve upon the gain and SLL of the full array structures while also providing a consistently reduced average mutual coupling value. PSO also produces an optimised array configuration that provides the most resilience to the application of beam steering, with improved gain and SLL values when compared with the full array. Alternatively, NMSA could be useful for fixed beam applications for the given array structures. It converges quickly, achieves optimisation targets, and provides the lowest average mutual coupling values. However, significant degradation with beam steering application limits its utility. Areas for future research have also been suggested, with focus on, tuning of optimisation algorithms and a generalized framework for the reduction of mutual coupling in sparse arrays.

REFERENCES

[1] H. Krim and M. Viberg, "Two decades of array signal processing research: The parametric approach," *IEEE Signal Process. Mag.*, vol. 13, no. 4, pp. 67–94, Jul. 1996, doi: 10.1109/79.526899.

[2] T. S. Rappaport et al., "Millimeter wave mobile communications for 5G cellular: It will Work!" *IEEE Access*, vol. 1, pp. 335–349, 2013, doi: 10.1109/ACCESS.2013.2260813.

[3] B. Friedlander and A. J. Weiss, "Direction finding in the presence of mutual coupling," *IEEE Trans. Antennas Propag.*, vol. 39, no. 3, pp. 273–284, Mar. 1991, doi: 10.1109/8.76322.

[4] C.-B. Moon, J.-W. Jeong, K.-H. Nam, Z. Xu, and J.-S. Park, "Design and analysis of a thinned phased array antenna for 5G wireless applications," *Int. J. Antennas Propag.*, vol. 2021, Oct. 2021, Art. no. 3039183, doi: 10.1155/2021/3039183.

[5] F. Roos et al., "Compressed sensing based single snapshot DoA estimation for sparse MIMO radar arrays," in *Proc. 12th German Microw. Conf. (GeMiC)*, Stuttgart, Germany, 2019, pp. 75–78, doi: 10.23919/GEMIC.2019.8698136.

[6] P. Minvielle, E. Tantar, A.-A. Tantar, and P. Berisset, "Sparse antenna array optimization with the cross-entropy method," *IEEE Trans. Antennas Propag.*, vol. 59, no. 8, pp. 2862–2871, Aug. 2011, doi: 10.1109/TAP.2011.2158941.

[7] A. Di Serio, P. Hügler, F. Roos, and C. Waldschmidt, "2-D MIMO radar: A Method for array performance assessment and design of a planar antenna array," *IEEE Trans. Antennas Propag.*, vol. 68, no. 6, pp. 4604–4616, Jun. 2020, doi: 10.1109/TAP.2020.2972643.

[8] Y. Bresler and A. Macovski, "On the number of signals resolvable by a uniform linear array," *IEEE Trans. Acoust., Speech, Signal Process.*, vol. 34, no. 6, pp. 1361–1375, Dec. 1986, doi: 10.1109/TASSP.1986.1164973.

[9] A. Moffet, "Minimum-redundancy linear arrays," *IEEE Trans. Antennas Propag.*, vol. 16, no. 2, pp. 172–175, Mar. 1968, doi: 10.1109/TAP.1968.1139138.

[10] G. S. Bloom and S. W. Golomb, "Applications of numbered undirected graphs," *Proc. IEEE*, vol. 65, no. 4, pp. 562–570, Apr. 1977, doi: 10.1109/PROC.1977.10517.

[11] Y. D. Zhang, M. G. Amin, and B. Himed, "Sparsity-based DOA estimation using co-prime arrays," in *Proc. IEEE Int. Conf. Acoust., Speech Signal Process.*, 2013, pp. 3967–3971, doi: 10.1109/ICASSP.2013.6638403.

[12] S. Qin, Y. D. Zhang, and M. G. Amin, "Generalized coprime array configurations for direction-of-arrival estimation," *IEEE Trans. Signal Process.*, vol. 63, no. 6, pp. 1377–1390, Mar. 2015, doi: 10.1109/TSP.2015.2393838.

[13] P. Pal and P. P. Vaidyanathan, "Nested arrays: A novel approach to array processing with enhanced degrees of freedom," *IEEE Trans. Signal Process.*, vol. 58, no. 8, pp. 4167–4181, Aug. 2010, doi: 10.1109/TSP.2010.2049264.

[14] C.-L. Liu and P. P. Vaidyanathan, "Super nested arrays: Linear sparse arrays with reduced mutual coupling—Part I: Fundamentals," *IEEE Trans. Signal Process.*, vol. 64, no. 15, pp. 3997–4012, Aug. 2016, doi: 10.1109/TSP.2016.2558159.

[15] A. Patwari, "Sparse linear antenna arrays: A review," in *Antenna Systems*. London, U.K.: IntechOpen, 2021, doi: 10.5772/intechopen.99444.

[16] A. Kedar, *Sparse Phased Array Antennas: Theory and Applications*. Norwood, MA, USA: Artech, 2022.

[17] P. Rocca, G. Oliveri, R. J. Mailloux, and A. Massa, "Unconventional phased array architectures and design methodologies—A review," in *Proc. IEEE*, vol. 104, no. 3, pp. 544–560, Mar. 2016, doi: 10.1109/JPROC.2015.2512389.

[18] I. Aboumahmoud, A. Muqaibel, M. Alhassoun, and S. Alawsh, "A review of sparse sensor arrays for two-dimensional direction-of-arrival estimation," *IEEE Access*, vol. 9, pp. 92999–93017, 2021, doi: 10.1109/ACCESS.2021.3092529.

[19] I. Gupta and A. Ksienski, "Effect of mutual coupling on the performance of adaptive arrays," *IEEE Trans. Antennas Propag.*, vol. 31, no. 5, pp. 785–791, Sep. 1983, doi: 10.1109/TAP.1983.1143128.

[20] M. K. Ozdemir, H. Arslan, and E. Arvas, "Mutual coupling effect in multiantenna wireless communication systems," in *Proc. IEEE Glob. Telecomm. Conf. (IEEE Cat. No.03CH37489)*, San Francisco, CA, USA, 2003, pp. 829–833, doi: 10.1109/GLOCOM.2003.1258355.

[21] C. Bencivenni, M. V. Ivashina, R. Maaskant, and J. Wettergren, "Design of maximally sparse antenna arrays in the presence of mutual coupling," *IEEE Antennas Wireless Propag. Lett.*, vol. 14, pp. 159–162, 2015, doi: 10.1109/LAWP.2014.2357450.

[22] E. BouDaher, F. Ahmad, M. G. Amin, and A. Hoorfar, "Mutual coupling effect and compensation in non-uniform arrays for direction-of-arrival estimation," *Digit. Signal Process.*, vol. 61, pp. 3–14, Feb. 2017, doi: 10.1016/j.dsp.2016.06.005.

[23] E. BouDaher, F. Ahmad, M. G. Amin, and A. Hoorfar, "Effect of mutual coupling on direction-of-arrival estimation using sparse dipole arrays," in *Proc. IEEE Int. Symp. Antennas Propag. (APSURSI)*, 2016, pp. 2189–2190, doi: 10.1109/APS.2016.7696801.

[24] H.-S. Lui, H. T. Hui, and M. S. Leong, "A note on the mutual-coupling problems in transmitting and receiving antenna arrays," *IEEE Antennas Propag. Mag.*, vol. 51, no. 5, pp. 171–176, Oct. 2009, doi: 10.1109/MAP.2009.5432083.

[25] C.-L. Liu and P. P. Vaidyanathan, "Super nested arrays: Linear sparse arrays with reduced mutual coupling—Part II: High-order extensions," *IEEE Trans. Signal Process.*, vol. 64, no. 16, pp. 4203–4217, Aug. 2016, doi: 10.1109/TSP.2016.2558167.

[26] J. He, L. Li, and T. Shu, "Sparse nested arrays with spatially spread orthogonal dipoles: High accuracy passive direction finding with less mutual coupling," *IEEE Trans. Aerosp. Electron. Syst.*, vol. 57, no. 4, pp. 2337–2345, Aug. 2021, doi: 10.1109/TAES.2021.3054056.

[27] W. Zheng, X. Zhang, Y. Wang, J. Shen, and B. Champagne, "Padded coprime arrays for improved DOA estimation: Exploiting hole representation and filling strategies," *IEEE Trans. Signal Process.*, vol. 68, pp. 4597–4611, Jul. 2020, doi: 10.1109/TSP.2020.3013389.

[28] J. Li, Y. Li, and X. Zhang, "Two-dimensional off-grid DOA estimation using unfolded parallel coprime array," *IEEE Commun. Lett.*, vol. 22, no. 12, pp. 2495–2498, Dec. 2018, doi: 10.1109/LCOMM.2018.2872955.

[29] C.-L. Liu and P. P. Vaidyanathan, "Hourglass arrays and other novel 2-D sparse arrays with reduced mutual coupling," *IEEE Trans. Signal Process.*, vol. 65, no. 13, pp. 3369–3383, Jul. 2017, doi: 10.1109/TSP.2017.2690390.

[30] S. Nakamura, S. Iwazaki, and K. Ichige, "An optimum 2D sparse array configuration with reduced mutual coupling," in *Proc. Int. Symp. Antennas Propag. (ISAP)*, 2018, pp. 1–2.

[31] A. Kedar, "Deterministic synthesis approach for linear sparse array antennas," *IEEE Trans. Antennas Propag.*, vol. 68, no. 9, pp. 6667–6674, Sep. 2020, doi: 10.1109/TAP.2020.2985155.
[32] Z. Zheng, C. Yang, W.-Q. Wang, and H. C. So, "Robust DOA estimation against mutual coupling with nested array," *IEEE Signal Process. Lett.*, vol. 27, pp. 1360–1364, Jul. 2020, doi: 10.1109/LSP.2020.3011314.
[33] E. BouDaher and A. Hoorfar, "Comparison of nature-inspired techniques in design optimization of non-uniformly spaced arrays in the presence of mutual coupling," *Digit. Signal Process.*, vol. 105, Oct. 2020, Art. no. 102780.
[34] E. Saudi, F. Y. Zulkifli, Basari, and E. T. Rahardjo, "A hybrid technique linear sparse array antenna design approach," *Proc. Int. Symp. Antennas Propag. (ISAP)*, Hobart, TAS, Australia, 2015, pp. 1–3.
[35] P. Angeletti and G. Toso, "Optimal amplitude–density synthesis of linear aperiodic arrays," *IEEE Trans. Antennas Propag.*, vol. 71, no. 6, pp. 4903–4918, Jun. 2023, doi: 10.1109/TAP.2023.3254215.
[36] X.-S. Yang, *Nature-Inspired Optimization Algorithms*. Amsterdam, The Netherlands: Elsevier, 2014.
[37] J. H. Holland, *Adaptation in Natural and Artificial Systems: An Introductory Analysis with Applications to Biology, Control, and Artificial Intelligence*. Cambridge, MA, USA: The MIT Press, 1992.
[38] N. Hansen and A. Ostermeier, "Adapting arbitrary normal mutation distributions in evolution strategies: The covariance matrix adaptation," in *Proc. IEEE Int. Conf. Evol. Comput.*, 1996, pp. 312–317, doi: 10.1109/ICEC.1996.542381.
[39] J. Kennedy and R. Eberhart, "Particle swarm optimization," in *Proc. Int. Conf. Neural Netw. (ICNN'95)*, 1995, pp. 1942–1948, doi: 10.1109/ICNN.1995.488968.
[40] D. C. Sorensen, "Newton's method with a model trust region modification," *SIAM J. Numer. Anal.*, vol. 19, no. 2, pp. 409–426, 1982.
[41] J. A. Nelder and R. Mead, "A simplex method for function minimization," *Comput. J.*, vol. 7, no. 4, pp. 308–313, 1965.
[42] J. E. Dennis Jr. and J. J. Moré, "Quasi-Newton methods, motivation and theory," *SIAM Rev.*, vol. 19, no. 1, pp. 46–89, Jan. 1977, doi: 10.1137/1019005.
[43] M. J. D. Powell, "An efficient method for finding the minimum of a function of several variables without calculating derivatives," *Comput. J.*, vol. 7, no. 2, pp. 155–162, Feb. 1964, doi: 10.1093/comjnl/7.2.155.
[44] H. Singh, H. L. Sneha, and R. M. Jha, "Mutual coupling in phased arrays: A review," *Int. J. Antennas Propag.*, vol. 2013, Apr. 2013, Art. no. 348123, doi: 10.1155/2013/348123.
[45] A. Das, D. Mandal, S. P. Ghoshal, and R. Kar, "An efficient side lobe reduction technique considering mutual coupling effect in linear array antenna using BAT algorithm," *Swarm Evol. Comput.*, vol. 35, pp. 26–40 Aug. 2017, doi: 10.1016/j.swevo.2017.02.004.
[46] Z. Yang, Q. Shen, W. Liu, Y. C. Eldar, and W. Cui, "High-order cumulants based sparse array design via fractal geometries—Part II: Robustness and mutual coupling," *IEEE Trans. Signal Process.*, vol. 71, pp. 343–357, Feb. 2023, doi: 10.1109/TSP.2023.3244667.
[47] Z. Zheng, W.-Q. Wang, Y. Kong, and Y. D. Zhang, "MISC array: A new sparse array design achieving increased degrees of freedom and reduced mutual coupling effect," *IEEE Trans. Signal Process.*, vol. 67, no. 7, pp. 1728–1741, Apr. 2019, doi: 10.1109/TSP.2019.2897954.
[48] R. Rajamäki and V. Koivunen, "Sparse active rectangular array with few closely spaced elements," *IEEE Signal Process. Lett.*, vol. 25, no. 12, pp. 1820–1824, Dec. 2018, doi: 10.1109/LSP.2018.2876066.
[49] A. Raza, W. Liu, and Q. Shen, "Thinned coprime array for second-order difference co-array generation with reduced mutual coupling," *IEEE Trans. Signal Process.*, vol. 67, no. 8, pp. 2052–2065, Apr. 2019, doi: 10.1109/TSP.2019.2901380.
[50] W. Shi, S. A. Vorobyov, and Y. Li, "ULA fitting for sparse array design," *IEEE Trans. Signal Process.*, vol. 69, pp. 6431–6447, Nov. 2021, doi: 10.1109/TSP.2021.3125609.
[51] X. Zhao, Q. Yang, and Y. Zhang, "Study on the trend of the sparsity of phased antenna array versus steering range," in *Proc. IEEE Int. Symp. Antennas Propag. North Am. Radio Sci. Meet.*, Montreal, QC, Canada, 2020, pp. 367–368, doi: 10.1109/IEEECONF35879.2020.9330102.
[52] Y. Li and Y. Li, "Investigation on SIW slot antenna array with beam scanning ability," *Int. J. Antennas Propag.*, vol. 2019, Jan. 2019, Art. no. 8293624, doi: 10.1155/2019/8293624.
[53] A. Kedar and L. P. Ligthart, "Wide scanning characteristics of sparse phased array antennas using an analytical expression for directivity," *IEEE Trans. Antennas Propag.*, vol. 67, no. 2, pp. 905–914, Feb. 2019, doi: 10.1109/TAP.2018.2880006.
[54] D. H. Wolpert and W. G. Macready, "No free lunch theorems for optimization," *IEEE Trans. Evol. Comput.*, vol. 1, no. 1, pp. 67–82, Apr. 1997, doi: 10.1109/4235.585893.
[55] R. L. Haupt and M. Lanagan, "Reconfigurable antennas," *IEEE Antennas Propag. Mag.*, vol. 55, no. 1, pp. 49–61, Feb. 2013, doi: 10.1109/MAP.2013.6474484.
[56] L. Marnat, A. A. A. Carreno, D. Conchouso, M. G. Martı′nez, I. G. Foulds, and A. Shamim, "New movable plate for efficient millimeter wave vertical on-chip antenna," *IEEE Trans. Antennas Propag.*, vol. 61, no. 4, pp. 1608–1615, Apr. 2013, doi: 10.1109/TAP.2013.2241720.
[57] A. Zhuravlev, V. Razevig, S. Ivashov, A. Bugaev, and M. Chizh, "Experimental simulation of multi-static radar with a pair of separated movable antennas," in *Proc. IEEE Int. Conf. Microw., Commun., Antennas Electron. Syst. (COMCAS)*, Tel Aviv, Israel, 2015, pp. 1–5, doi: 10.1109/COMCAS.2015.7360379.
[58] Z. Lipeng, M. Wenyan, and Z. Rui, "Movable antennas for wireless communication: Opportunities and challenges," 2023, *arXiv:2306.02331*.
[59] Z. Lipeng, M. Wenyan, and Z. Rui, "Modeling and performance analysis for movable antenna enabled wireless communications," 2022, *arXiv:2210.05325*.
[60] C. Bencivenni, M. V. Ivashina, R. Maaskant, and J. Wettergren, "Synthesis of maximally sparse arrays using compressive sensing and full-wave analysis for global earth coverage applications," *IEEE Trans. Antennas Propag.*, vol. 64, no. 11, pp. 4872–4877, Nov. 2016.
[61] A. Patwari and G. R. Reddy, "1D direction of arrival estimation using root-MUSIC and ESPRIT for dense uniform linear arrays," in *Proc. 2nd IEEE Int. Conf. Recent Trends in Electron., Inf. Commun. Technol. (RTEICT)*, Bengaluru, India, 2017, pp. 667–672, doi: 10.1109/RTEICT.2017.8256681.
[62] F. Gu, L. Chi, Q. Zhang, and F. Zhu, "Single snapshot imaging method in multiple-input multiple-output radar with sparse antenna array," *IET Radar Sonar Navig.*, vol. 7, pp. 535–543, Jun. 2013, doi: 10.1049/iet-rsn.2011.0363.
[63] X. Hu, N. Tong, B. Song, S. Ding, and X. Zhao, "Joint sparsity-driven three-dimensional imaging method for multiple-input multiple-output radar with sparse antenna array," *IET Radar Sonar Navig.*, vol. 11, no. 5, pp. 709–720, May 2017, doi: 10.1049/iet-rsn.2016.0108.
[64] W. Shi, Y. Li, L. Zhao, and X. Liu, "Controllable sparse antenna array for adaptive beamforming," *IEEE Access*, vol. 7, pp. 6412–6423, 2019, doi: 10.1109/ACCESS.2018.2889877.
[65] C. Yan, P. Yang, Z. Xing, and S. Y. Huang, "Synthesis of planar sparse arrays with minimum spacing constraint," *IEEE Antennas Wireless Propag. Lett.*, vol. 17, pp. 1095–1098, 2018, doi: 10.1109/LAWP.2018.2833962.